Optimal electrode selection for multi-channel electroencephalogram based detection of auditory steady-state responses

Bram Van Dun[a] and Jan Wouters
ExpORL, Katholieke Universiteit Leuven, Herestraat 49/721, B-3000 Leuven, Belgium

Marc Moonen
ESAT-SCD/SISTA, Katholieke Universiteit Leuven, Kasteelpark Arenberg 10, B-3001 Leuven, Belgium

(Received 15 October 2008; revised 21 April 2009; accepted 23 April 2009)

Auditory steady-state responses (ASSRs) are used for hearing threshold estimation at audiometric frequencies. Hearing impaired newborns, in particular, benefit from this technique as it allows for a more precise diagnosis than traditional techniques, and a hearing aid can be better fitted at an early age. However, measurement duration of current single-channel techniques is still too long for clinical widespread use. This paper evaluates the practical performance of a multi-channel electroencephalogram (EEG) processing strategy based on a detection theory approach. A minimum electrode set is determined for ASSRs with frequencies between 80 and 110 Hz using eight-channel EEG measurements of ten normal-hearing adults. This set provides a near-optimal hearing threshold estimate for all subjects and improves response detection significantly for EEG data with numerous artifacts. Multi-channel processing does not significantly improve response detection for EEG data with few artifacts. In this case, best response detection is obtained when noise-weighted averaging is applied on single-channel data. The same test setup (eight channels, ten normal-hearing subjects) is also used to determine a minimum electrode setup for 10-Hz ASSRs. This configuration allows to record near-optimal signal-to-noise ratios for 80% of subjects.
© *2009 Acoustical Society of America.* [DOI: 10.1121/1.3133872]

PACS number(s): 43.64.Ri, 43.66.Yw, 43.66.Sr [BLM] Pages: 254–268

I. INTRODUCTION

Universal detection of infants with hearing loss is recommended before the age of 3 months (Joint Committee on Infant Hearing, 1995). As the number of hearing screened newborns grows worldwide, the need for objective audiometric techniques has greatly increased over the past decade. An appropriate clinical response to the need for rehabilitation of hearing problems is necessary. An effective treatment may consist of the use of a hearing aid. However, fitting of this device requires a frequency specific estimation of the newborn's hearing thresholds. These estimates can be provided using auditory steady-state response (ASSR) detection long before first behavioral thresholds can be obtained. Unfortunately, a reliable ASSR-based hearing threshold estimation procedure takes 45 min with adults and can last several hours with newborns (Luts *et al.*, 2006). The measured signals are often corrupted by artifacts due to the newborn's movements during measurement. The general aim is thus to increase robustness against artifacts and to reduce measurement time. Before actual studies can be carried out on infants, the proposed techniques are evaluated on adults. Behavioral hearing thresholds can easily be determined with adults and hence a reference is obtained for application in the infant population.

The ASSR is an electrophysiological response of the brain evoked by acoustic stimuli. These stimuli are generally based on amplitude modulated (AM) and/or frequency modulated (FM) sinusoidal carriers. The carriers stimulate specific parts of the cochlea, while the modulations activate certain parts of the auditory system. The appearance of the modulation frequency in the electroencephalogram (EEG) can be used as a label for the carrier frequency. The first significant ASSR study was conducted by Galambos *et al.* (1981) with modulation frequencies of 40 Hz. Subsequently, extensive research has shown that the ASSR can indeed provide an objective and frequency specific way to determine reliable hearing thresholds, both applicable to adults and infants [we refer to Picton *et al.* (2003) for an extensive overview].

Many research studies have focused on optimizing detection of ASSRs. First, different stimulus types have been investigated. AM and/or FM stimuli are most widely accepted (John *et al.*, 2001b). Other stimuli are stimuli with exponential modulation envelopes (John *et al.*, 2002), broadband and band-limited noise (John *et al.*, 2003), stimuli composed of several carriers modulated with the same modulation frequency (Stürzebecher *et al.*, 2001), and complex stimuli with broader frequency spectra (Riquelme *et al.*, 2006; Stürzebecher *et al.*, 2006). In general, responses are more difficult to detect when stimuli become more frequency specific. Second, normal averaging has been compared with weighted averaging and artifact rejection (John *et al.*, 2001a). Third, the possibility to increase ASSR detection ef-

[a]Also at ESAT-SCD/SISTA, Katholieke Universiteit Leuven, Kasteelpark Arenberg 10, B-3001 Leuven, Belgium. Author to whom correspondence should be addressed. Electronic mail: bram.vandun@med.kuleuven.be

ficiency by means of multi-channel EEG recordings has been evaluated (van der Reijden *et al.*, 2004; Van Dun *et al.*, 2007a, 2007b). Last, several statistical decision criteria have been studied: tests that use spectral phase information, spectral amplitude information, or both; tests that evaluate only the first harmonic of the response (Cebulla *et al.*, 2001; Dobie and Wilson, 1996) and recently, tests that include higher harmonics for response detection (Cebulla *et al.*, 2006).

Most studies are based on EEG data obtained from subjects who are instructed to relax or sleep. In practice, however, and especially with newborns, numerous artifacts prevent a successful measurement unless one takes appropriate measures against these artifacts. This can be achieved using artifact rejection or weighted averaging (John *et al.*, 2001a). Data blocks severely corrupted with artifacts are entirely discarded or are not allowed to contribute much to the final result. The disadvantage of these techniques is measurement time. Therefore, other techniques have been researched that are more robust against artifacts. These techniques should allow detection of significantly more responses in the presence of artifactual energy in the EEG without extending measurement time.

A well-chosen electrode derivation makes response registration easier. The Cz-Oz or Cz-neck derivations are the most commonly used derivations for adults because mean ASSR thresholds are smaller for these derivations (John *et al.*, 2001a; Lins and Picton, 1995; Luts and Wouters, 2005). This is confirmed for Cz-Oz derivations by van der Reijden *et al.* (2004).

A multi-channel setup is used to search for derivations offering the largest signal-to-noise ratio (SNR) values and thus the smallest ASSR thresholds for adults. This Cz-Oz derivation does not always guarantee the largest SNR and sometimes other derivations (for example, Cz-mastoid, Cz-Pz, and Cz-neck) offer larger SNRs. This is supported by observations that ASSR thresholds (and their SNRs) show large variations across subjects (John *et al.*, 2001a; Lins and Picton, 1995; Luts and Wouters, 2005). However, the derivation with the largest SNR is subject-dependent and cannot be predicted beforehand. Hence, EEG data recorded using multiple derivations simultaneously, combined with appropriate multi-channel processing, are required to select the "best" channel (or combination of channels) for as many subjects as possible.

The first part of this introduction focuses on hearing threshold estimation using ASSRs with modulation frequencies between 80 and 110 Hz. These responses are generated mainly in the brainstem. The problem statement is not restricted to this frequency range however. It would be interesting to focus on multi-channel EEG data containing ASSRs with lower modulation frequencies, mainly generated in the auditory cortex. The amplitude of these responses varies more with subject, modulation frequency, and state of arousal. Moreover, generally more noise is obscuring the response in lower-frequency regions due to other brain processes. ASSRs to lower frequencies may be more closely related to actual processes of speech understanding. Speech is a complex acoustic waveform containing different spectral and temporal cues for intelligibility. Lower modulation frequencies consisting of envelope information (with modulation frequencies below 20 Hz) appear critical for speech intelligibility (Drullman *et al.*, 1994a, 1994b; Saberi and Perrott, 1999; Shannon *et al.*, 1995). Earlier publications mention ASSRs at frequencies between 2 and 40 Hz [for example, Cohen *et al.* (1991); Galambos *et al.* (1981); Picton *et al.* (1987)]. Recent studies introduce envelope-following responses to slow rates using AM noise (Purcell *et al.*, 2004) and spoken sentences (Aiken and Picton, 2008). Alaerts *et al.* (2009) linked cortical ASSRs at low frequencies to behavioral outcomes of speech processing. ASSRs are significantly correlated with speech reception thresholds for phonemes and sentences in noise, independent of intensity level. Trends of increased responses around 10 and/or 20 Hz are found. Therefore, it is decided in this study to use 10 Hz as a representative for cortical ASSRs.

This paper evaluates practical performance of a multi-channel processing strategy based on a detection theory approach when applied to adults. It is based on eight-channel EEG measurements of ten normal-hearing adults. The results serve as an intermediate step for application of multi-channel processing to infants. First, the EEG derivation with best estimation of behavioral hearing threshold for ASSRs originating mainly from the brainstem is determined (modulation frequencies between 80 and 110 Hz in this paper). For ASSRs originating mainly from the auditory cortex (a modulation frequency of 10 Hz in this paper), the EEG derivation providing largest SNR is determined. Then, the minimum EEG-channel combination is determined for brainstem ASSRs with a near-optimal estimation of behavioral hearing thresholds for as many subjects as possible. As a practical application of this result, robustness of this minimum set to artifacts is investigated. Similarly, for auditory cortex ASSRs, the minimum EEG-channel combination is determined that provides near-optimal SNRs for a maximum number of subjects.

II. THEORETICAL BACKGROUND

ASSRs are difficult to detect due to noise originating from sources both inside and outside the skull. As a result, clinical measurements can last an unacceptably long period of time. Specifically designed signal processing techniques may reduce this measurement time. These techniques may increase the robustness against energetic artifacts that could suddenly emerge. These artifacts appear frequently in ASSR measurements.

This section describes a multi-channel signal processing technique appropriate for ASSR detection. Its rationale is based on a concept from detection theory, the *sufficient statistic*. This sufficient statistic can exploit spatio-temporal information present in the EEG measurements. A more extensive description can be found in Van Dun *et al.* (2009).

A. ASSR data model

A general ASSR data model can be given as

$$\boldsymbol{Z} = \alpha \boldsymbol{S}\boldsymbol{D}^T + \boldsymbol{N}, \tag{1}$$

with $\boldsymbol{Z}^{n\times m}$ an observation matrix, α a scalar representing the ASSR source amplitude proportional to the applied stimulus intensity, $\boldsymbol{S}^{n\times 2}$ a desired signal matrix with columns representing the ASSR (sinusoid and cosinusoid, oscillating at the known modulation frequency), $\boldsymbol{D}^{m\times 2}$ a steering matrix, $\boldsymbol{N}^{n\times m}$ an additive noise matrix, n the number of data points, and m the number of measured EEG-channels.

In Eq. (1), given only $\boldsymbol{Z}$ and $\boldsymbol{S}$, $\alpha\boldsymbol{D}$ and $\boldsymbol{N}$ can be estimated using a QR-factorization:

$$\overbrace{[\boldsymbol{s}_1^{n\times 1} \quad \boldsymbol{s}_s^{n\times 1}}^{\boldsymbol{S}} \quad \boldsymbol{Z}^{n\times m}] = \boldsymbol{Q}^{n\times(m+2)}\boldsymbol{R}^{(m+2)\times(m+2)}, \tag{2}$$

with

$$\boldsymbol{Q} = [\boldsymbol{s}_1 \quad \boldsymbol{s}_2 \quad \boldsymbol{Q}_*^{n\times m}], \quad \boldsymbol{R} = \begin{bmatrix} 1 & 0 & \hat{\boldsymbol{d}}_1^T \\ 0 & 1 & \hat{\boldsymbol{d}}_2^T \\ \boldsymbol{0} & \boldsymbol{0} & \boldsymbol{R}_*^{m\times m} \end{bmatrix}. \tag{3}$$

$\boldsymbol{Z}$ can then be written as

$$\boldsymbol{Z} = \overbrace{[\boldsymbol{s}_1 \quad \boldsymbol{s}_2]}^{\boldsymbol{S}} \overbrace{\begin{bmatrix} \hat{\boldsymbol{d}}_1^T \\ \hat{\boldsymbol{d}}_2^T \end{bmatrix}}^{\hat{\boldsymbol{D}}^T} + \overbrace{\boldsymbol{Q}_*\boldsymbol{R}_*}^{\hat{\boldsymbol{N}}}, \tag{4}$$

where $\hat{\boldsymbol{D}}$ and $\hat{\boldsymbol{N}}$ are the estimates provided for $\alpha\boldsymbol{D}$ and $\boldsymbol{N}$.

A physical interpretation is given here. The ASSR generator has an unknown source amplitude α, which depends on stimulus level. After propagation through the skull, the distribution of the recorded ASSR on the electrodes can be described by steering matrix $\boldsymbol{D}$. This steering matrix $\boldsymbol{D}$, unlike the additive EEG noise, is usually assumed to be stationary as it is only a representation of source position, directivity pattern, electrode positions, and propagation attenuation from source to electrode. Physically, no measurable delay occurs between ASSR source and electrodes (order of nanoseconds). Therefore the ASSR delay difference and hence the ASSR phase difference between electrodes are assumed to be zero. On the other hand, the delay between ASSR stimulus and response is measurable (order of milliseconds), but unknown to the observer as it depends on several physical parameters of the subject. The ASSR phase φ at the electrodes is thus unknown but equal in all channels.

Equation (1) can then be rewritten as

$$\boldsymbol{Z} = \alpha\boldsymbol{S}\overbrace{\begin{bmatrix} \cos\varphi \\ \sin\varphi \end{bmatrix}}^{\boldsymbol{D}^T}\boldsymbol{d}^T + \boldsymbol{N} \tag{5}$$

$$= \alpha\boldsymbol{s}\boldsymbol{d}^T + \boldsymbol{N}, \tag{6}$$

where now $\boldsymbol{s}$ and $\boldsymbol{d}$ are vectors, and φ corresponds to the ASSR phase.

The phase φ can be estimated based on Eq. (4),

$$\hat{\varphi} = \arg\left\{ \max_{\varphi} [\cos\varphi \ \sin\varphi]\hat{\boldsymbol{D}}^T(\hat{\boldsymbol{N}}^T\hat{\boldsymbol{N}})^{-1}\hat{\boldsymbol{D}}\begin{bmatrix} \cos\varphi \\ \sin\varphi \end{bmatrix} \right\}. \tag{7}$$

The estimated phase $\hat{\varphi}$ expresses the direction that maximizes the projection of the observation matrix $\boldsymbol{Z}$ onto the desired signal $\boldsymbol{S}[\cos\varphi \ \sin\varphi]^T$ as $\hat{\boldsymbol{D}} = \boldsymbol{Z}^T\boldsymbol{S}$. Based on $\hat{\varphi}$, a rotation transformation is applied to $\hat{\boldsymbol{D}}$,

$$\hat{\boldsymbol{d}} = \hat{\boldsymbol{D}}\begin{bmatrix} \cos\hat{\varphi} \\ \sin\hat{\varphi} \end{bmatrix}, \tag{8}$$

such that the estimated steering matrix $\hat{\boldsymbol{D}}$ is transformed into an estimated steering vector $\hat{\boldsymbol{d}}$.

A spatio-temporal noise covariance matrix $\boldsymbol{K}^{mn\times mn}$ can be defined as

$$\boldsymbol{K} = \mathcal{E}\{\boldsymbol{n}\boldsymbol{n}^T\}, \tag{9}$$

with $\boldsymbol{n} = \mathrm{vec}(\boldsymbol{N})$. Here $\mathcal{E}\{\cdot\}$ is the expected value operator and the vec$(\cdot)$ operator stacks the columns of a matrix $\boldsymbol{X}$ into one column vector $\boldsymbol{x} = \mathrm{vec}(\boldsymbol{X})$.

If spatial and temporal correlations are separable, as will be observed here, the spatio-temporal noise covariance matrix $\boldsymbol{K}$ can be written as (Johnson and Dudgeon, 1993)

$$\boldsymbol{K} = \boldsymbol{K}_{\mathrm{spat}} \otimes \boldsymbol{K}_{\mathrm{temp}}, \tag{10}$$

where $\otimes$ represents the Kronecker product, with a spatial noise covariance matrix $\boldsymbol{K}_{\mathrm{spat}}^{m\times m}$, representing noise correlation across the different channels,

$$\boldsymbol{K}_{\mathrm{spat}} = \mathcal{E}\{\boldsymbol{N}^T\boldsymbol{N}\}, \tag{11}$$

and a temporal noise covariance matrix $\boldsymbol{K}_{\mathrm{temp}}^{n\times n}$, representing correlation of noise samples within the same channel,

$$\boldsymbol{K}_{\mathrm{temp}} = \mathcal{E}\{\boldsymbol{N}\boldsymbol{N}^T\}. \tag{12}$$

Based on Eq. (4) the noise covariance matrices can be estimated as

$$\hat{\boldsymbol{K}}_{\mathrm{spat}} = \hat{\boldsymbol{N}}^T\hat{\boldsymbol{N}}, \quad \hat{\boldsymbol{K}}_{\mathrm{temp}} = \hat{\boldsymbol{N}}\hat{\boldsymbol{N}}^T. \tag{13}$$

B. Detection theory: Detecting signals with unknown amplitude in noise

Detection theory is a means to quantify the ability to discern between signal and noise (Green and Swets, 1966). Here, a sufficient statistic $\Upsilon(z)$ is defined as

$$\Upsilon(z) = z^T\boldsymbol{K}^{-1}\tilde{\boldsymbol{s}}, \tag{14}$$

with a target signal $\tilde{\boldsymbol{s}}$ having an unknown amplitude α, and $\boldsymbol{K}$ the covariance matrix of the noise $\boldsymbol{n}$ that corrupts the observation vector z,

$$z = \alpha\tilde{\boldsymbol{s}} + \boldsymbol{n}. \tag{15}$$

A sufficient statistic theoretically captures best the amount of useful target signal $\tilde{\boldsymbol{s}}$ in the observation vector z. A decision threshold η for $\Upsilon(z)$ can be determined by specifying a false-alarm probability. This threshold η decides whether the observation vector z contains the target signal $\tilde{\boldsymbol{s}}$ or not.

C. A detection theory framework for ASSR processing

The ASSR signal model of Eq. (6) can be reformulated as

$$z = \alpha\overbrace{\boldsymbol{d}\otimes\boldsymbol{s}}^{\tilde{\boldsymbol{s}}} + \boldsymbol{n}, \tag{16}$$

with $z=\mathrm{vec}(\boldsymbol{Z})$ and $\boldsymbol{n}=\mathrm{vec}(\boldsymbol{N})$, respectively.

The sufficient statistic [Eq. (14)] can be applied here by identifying Eq. (15) with Eq. (16),

$$\Upsilon_A(z)=z^T\boldsymbol{K}^{-1}\tilde{\boldsymbol{s}}. \tag{17}$$

Replacing $\boldsymbol{K}$ by using Eq. (10), and $\tilde{\boldsymbol{s}}$ by using Eq. (16), Eq. (17) becomes

$$\Upsilon_A(z)=z^T(\boldsymbol{K}_{\mathrm{spat}}\otimes\boldsymbol{K}_{\mathrm{temp}})^{-1}(\boldsymbol{d}\otimes\boldsymbol{s}) \tag{18}$$

$$=\boldsymbol{s}^T\boldsymbol{K}_{\mathrm{temp}}^{-T}\boldsymbol{Z}\boldsymbol{K}_{\mathrm{spat}}^{-1}\boldsymbol{d}. \tag{19}$$

Substituting the estimates based on Eqs. (2)–(4), (7), (8), and (13) leads to a sufficient statistic $\hat{\Upsilon}_A(z)$ suitable for ASSR detection,

$$\hat{\Upsilon}_A(z)=[\cos\hat{\varphi}\ \sin\hat{\varphi}]\boldsymbol{S}^T\hat{\boldsymbol{K}}_{\mathrm{temp}}^{-T}\boldsymbol{Z}\hat{\boldsymbol{K}}_{\mathrm{spat}}^{-1}\hat{\boldsymbol{D}}\begin{bmatrix}\cos\hat{\varphi}\\ \sin\hat{\varphi}\end{bmatrix}. \tag{20}$$

When the EEG (noise) is stationary over all channels throughout the measurement, the covariance matrix $\boldsymbol{K}$ is constant too. When noise characteristics change over time, $\boldsymbol{K}$ cannot be considered constant anymore and Eq. (20) needs to be modified. If noise in $\boldsymbol{Z}$ is stationary only in blocks of T samples (rows) and uncorrelated between such blocks, then $\Upsilon_A(z)$ can be calculated as the sum of the sufficient statistics $\Upsilon_{A,i}(z_i)$ for the individual blocks $\boldsymbol{Z}_i$, i.e.,

$$\Upsilon_A(z)=\sum_{i=1}^{n/T}\boldsymbol{s}_i^T\boldsymbol{K}_{\mathrm{temp},i}^{-T}\boldsymbol{Z}_i\boldsymbol{K}_{\mathrm{spat},i}^{-1}\boldsymbol{d} \tag{21}$$

$$=\sum_{i=1}^{n/T}\Upsilon_{A,i}(z_i). \tag{22}$$

For each $\Upsilon_{A,i}(z_i)$ an approximation as in Eq. (20) can be used.

D. Detection using fast Fourier transformation

In many ASSR studies an objective procedure is developed where a fast Fourier transformation (FFT) analysis is carried out prior to response detection (John and Picton, 2000; Lins and Picton, 1995; Luts *et al.*, 2006; Valdes *et al.*, 1997). Detection is based on the ratio between response power P_r at the modulation frequency and mean noise power σ^2 in M neighboring frequency bins at each side,

$$\frac{P_r}{\sigma^2}=\frac{a_{\mathrm{response}}^2}{\frac{1}{M}\sum_{p=1}^{M}a_{\mathrm{noise},p}^2}, \tag{23}$$

with a_{response} the amplitude at the modulation frequency and $a_{\mathrm{noise},p}$ the noise amplitude in the pth adjacent frequency bin (John and Picton, 2000).

For brainstem responses (with modulation frequencies between 80 and 110 Hz), M is taken equal to 120 (approximately 3.7 Hz on each side). For auditory cortex responses (10 Hz), M is taken equal to 60 (approximately 1.85 Hz on each side).

III. METHODS

Two studies are described here: one based on ASSRs mainly evoked in the brainstem (modulation frequencies between 80 and 110 Hz) and one on ASSRs mainly evoked in the auditory cortex (10 Hz).

The 80–110-Hz range is the frequency region of interest for hearing threshold determination (Picton *et al.*, 2003). Several studies focus on the sources of these ASSRs. Herdman *et al.* (2002) suggested that 88-Hz ASSRs are mainly generated in the brainstem. Kuwada *et al.* (2002) indicated that ASSRs with modulation frequencies below 80 Hz mainly originate in the auditory cortex. Above 80 Hz, there appear to be at least two generators that are likely subcortical. This is confirmed by Purcell *et al.* (2004) who used response latencies to derive source locations. They concluded that for modulation frequencies above 75 Hz, most of the ASSR is generated in the brainstem. Above 95 Hz, the source lies entirely in the brainstem. As a result, in this paper responses to stimuli modulated with frequencies between 80 and 110 Hz are referred to as "responses mainly evoked in the brainstem."

The modulation frequency of 10 Hz is chosen because of its relevance for speech envelope modulations and speech perception (Drullman *et al.*, 1994a, 1994b; Saberi and Perrott, 1999; Shannon *et al.*, 1995). When lowering the modulation frequency of the stimulus, the main source of the ASSR shifts to the auditory cortex. According to Herdman *et al.* (2002), the main source can be found in the auditory cortex, but a source originating from the brainstem may still be present. This is supported by Purcell *et al.* (2004), showing that the brainstem still contributes at lower modulation frequencies, but the main source of the low-frequency ASSR is located in the auditory cortex. Responses to 10 Hz-modulated stimuli are in this paper referred to as "responses mainly evoked in the auditory cortex."

For both studies, 10 normal-hearing subjects (8 male, 2 female) with mean age 28.2 years (range 22–32 years) have been selected. Their hearing thresholds do not exceed 20 dB hearing level (HL) on the octave audiometric frequencies. All experiments have been carried out in a double-walled soundproof room with Faraday cage. Subjects have been instructed to lie down on a bed and relax or sleep for the brainstem study in Sec. III A and to stay awake while watching a movie for the auditory cortex study in Sec. III B. Lights have been switched off. This procedure has been repeated a number of weeks later to collect both test and retest data.

Kendall jelly snap electrodes have been placed on the positions described in Table I adhering to the international 10-20 system (Malmivuo and Plonsey, 1995). This configuration has been chosen similar to van der Reijden *et al.* (2004) with some extra channels added to ensure a symmetrical configuration of all electrodes. They have been placed on the subject's scalp after the skin has been abraded with Nuprep abrasive skin prepping gel. A conductive paste has been used to keep electrodes in place and to avoid that inter-electrode impedances exceed 5 kΩ at 30 Hz. Electrodes have been connected to a low-noise eight-channel Jaeger–Toennies amplifier. Each EEG-channel has been am-

TABLE I. Recording electrode positions for an eight-channel setup according to the international 10–20 system (Malmivuo and Plonsey, 1995). All channels are referenced to the reference electrode on top of the head (Cz). A graphical representation is shown in Fig. 2. The term "side" indicates on which hemisphere of the head the electrode is placed in the case it is not positioned on the middle line from front to back. In general, the sides can be "left" or "right." However, for ASSRs from the auditory cortex, being described in Sec. V (with stimuli referenced to the right ear), one refers to the sides as "ipsilateral" and "contralateral." The ipsilateral side is the side of stimulation.

Channel	Position	Side
1	Occiput (Oz)	
2	P4	R/I
3	P3	L/C
4	Right mastoid (M2)	R/I
5	Left mastoid (M1)	L/C
6	F4	R/I
7	F3	L/C
8	Forehead (Fpz)	
Reference	Vertex (Cz)	
Ground	Right clavicle	

plified ($\times 50\,000$) and bandpass filtered between 70 and 170 Hz (6 dB/octave) for the brainstem study in Sec. III A and between 1 and 30 Hz (6 dB/octave) for the auditory cortex study in Sec. III B. The sampling rate initially has been set to 1000 Hz, and afterward to 250 Hz using the *resample* function from MATLAB. The "accuracy" option has been set to $N=100$, which corresponds to an anti-aliasing (lowpass) finite impulse response filter with 800 taps. The MATLAB function compensates for filter delay. No artifact rejection was applied during testing, but a threshold has been determined offline that rejects around 10% of the recorded data blocks ("epochs") that exceed this artifact rejection threshold. All separate acoustic stimuli have been calibrated at 70-dB sound pressure level (SPL), using a Brüel & Kjær Sound Level Meter 2260 in combination with a 2-cc coupler DB0138. All stimuli have been presented to the subject, and amplified EEG signals have been recorded using the SOMA program from Van Dun *et al.* (2008) and an RME multichannel soundcard (RME, Germany).

It is important to note that all possible measures have been taken to avoid false responses not originating from statistical noise effects (the relative number of false responses originating from statistical noise is allowed to be 5%). Measures to avoid additional false responses include appropriate shielding of stimulus devices and electrodes, filtering prior to downsampling, and adequate separation of stimulus and electrode cables. Absence of false responses has been regularly checked by applying the stimuli to a simulated "deaf" subject (by blocking the ear canal of the subject using ear plugs).

A. Brainstem stimulation

Two combined stimuli with four 100% AM and 20% FM carrier frequencies each have been applied to each ear. The carrier frequencies are the same for both ears, namely, 0.5, 1, 2, and 4 kHz. Modulation frequencies have been chosen in the vicinity of 82, 90, 98, and 106 Hz for the left ear and 86, 94, 102, and 110 Hz for the right ear. These modulation frequencies have been adjusted to ensure that a non-fractional number of modulation cycles fits into one data block (epoch) of 1.024 s. For example, 82 Hz is converted to round(82×1.024)/1.024 Hz (John and Picton, 2000). Throughout the rest of this paper, the non-adjusted frequencies are referred to for conciseness.

For Secs. IV A and IV B, stimuli have been applied at an initial intensity of 60-dB SPL and lowered by 10 dB after a trial of approximately 10 min per intensity (36 sweeps, each sweep lasting 16.384 s). 10-dB SPL is the lowest intensity that has been applied. After EEG data collection, each separate channel, or each combination of channels, has been reduced to 32 sweeps, using an artifact rejection threshold that removes exactly 4 sweeps per channel (or per combination of channels). Artifact rejection for multi-channel data (i.e., a combination of channels) implies the removal of all simultaneous epochs over different channels to preserve correlation over simultaneous channels.

For the analysis of robustness against artifacts in Sec. IV C, EEG data from the previous paragraph are combined with extra measurements that emphasize occurrence of artifacts. Subjects have been instructed to be seated on a chair and to carry out a repeated series of movements in cycles of approximately 6 s. Meanwhile, the two acoustic stimuli described above have been applied at an intensity of 30-dB SPL. Measurements are 32 sweeps long. Movements have been carried out in the following order: turn the head up, down, left, and right. This procedure serves as a controlled generator of artifacts on all channels due to muscle activity and electrode cable movement. No artifact rejection has been applied as artifact rejection applied to single-channel artifact-rich EEG data would result in a significant reduction in withheld data and detected responses. When applied to multi-channel data, the number of withheld sweeps even would reduce to close to zero. A solution for excessive data rejection could be a less strict rejection threshold. This would negatively influence the detection performance for EEG data with few artifacts however. Also, the EEG quality is not known beforehand, which makes the choice of a fixed detection threshold difficult.

B. Auditory cortex stimulation

Contrary to brainstem stimulation, where multiple stimuli are applied simultaneously (Dimitrijevic *et al.*, 2002; Herdman and Stapells, 2001; Luts and Wouters, 2005), the use of such combined stimuli with modulation frequencies below 40 Hz has not been thoroughly documented yet (Armstrong and Stapells, 2007). Therefore, only one carrier frequency is modulated (instead of eight as in Sec. III A), which implies that only one ear is stimulated.

Speech-weighted Leuven intelligibility sentences test (LIST) noise from van Wieringen and Wouters (2008) has been 100% AM with an (adjusted) modulation frequency close to 10 Hz. The resulting stimulus has been applied with intensities of 50 and of 70-dB SPL to the ear with the smallest pure-tone average (PTA). Multi-channel EEG recordings

TABLE II. For each channel from Table I, mean SNRs (and standard deviations between brackets) of modulation frequencies (82, 90, 98, 106 Hz left, and 86, 94, 102, 110 Hz right) modulating the corresponding carrier frequency (500, 1000, 2000, and 4000 Hz, left and right) at a stimulus level of 30-dB SPL are displayed. Recording lengths are 32 sweeps after artifact rejection. Mean rms values (and standard deviations) of noise from each channel are shown at the right of the table.

Channel No.	Left (dB SNR)				Right (dB SNR)				rms (nV)
	500 Hz	1000 Hz	2000 Hz	4000 Hz	500 Hz	1000 Hz	2000 Hz	4000 Hz	
1 (Oz)	5.1 (6.5)	9.3 (2.8)	8.3 (4.0)	5.9 (6.3)	7.1 (5.2)	9.5 (7.0)	10.2 (3.9)	6.8 (5.6)	4.0 (1.3)
2 (P4)	4.2 (5.9)	5.8 (5.4)	4.9 (4.6)	3.1 (5.6)	5.9 (6.7)	9.7 (7.1)	10.1 (3.1)	6.0 (5.1)	2.5 (0.6)
3 (P3)	5.5 (4.7)	8.5 (4.6)	7.9 (4.1)	4.7 (4.9)	4.1 (5.3)	5.6 (6.3)	2.1 (5.4)	−0.4 (4.5)	2.7 (0.6)
4 (M2)	3.8 (7.6)	7.7 (5.0)	4.6 (6.6)	3.6 (7.0)	7.4 (7.7)	12.0 (5.5)	9.9 (2.5)	6.8 (4.7)	7.1 (3.1)
5 (M1)	4.5 (7.6)	10.2 (4.8)	8.1 (6.8)	5.1 (5.7)	4.5 (6.1)	7.2 (6.5)	8.7 (4.4)	3.4 (5.1)	6.1 (1.9)
6 (F4)	0.9 (2.2)	1.8 (5.0)	−0.5 (2.5)	−0.3 (4.7)	2.5 (3.1)	4.6 (4.5)	5.4 (3.0)	0.7 (3.2)	4.9 (3.0)
7 (F3)	2.5 (3.0)	5.0 (5.7)	1.9 (8.6)	0.5 (6.4)	3.0 (4.6)	3.9 (5.5)	2.9 (6.8)	0.6 (5.5)	3.7 (1.8)
8 (Fpz)	0.1 (4.8)	2.7 (5.1)	0.9 (5.1)	−1.3 (5.0)	1.8 (6.9)	3.5 (4.2)	3.3 (4.8)	0.7 (3.0)	4.9 (2.6)

have a length of 23 sweeps, reduced to 20 sweeps by removing epochs that exceed the calculated artifact rejection threshold (per channel or per combination of channels), similar to Sec. III A.

IV. RESULTS FOR BRAINSTEM ASSRS

This section addresses the following questions:

- What is the most appropriate single EEG-channel to record brainstem ASSRs?
- What is the most appropriate combination of multiple EEG-channels to record brainstem ASSRs?
- Are above conclusions influenced by the side of stimulation (left or right)?

All results in this section are based on the concept of *difference scores*. A difference score is the difference (in dB) between a ASSR threshold (in dB SPL) and a behavioral threshold (in dB SPL). The difference score is used in various ASSR studies (Dimitrijevic *et al.*, 2002; Herdman and Stapells, 2001; Luts and Wouters, 2005). In this study, it allows the available SNR data at six different intensities to be combined into one quantitative value which averages out the variation in behavioral thresholds between subjects and test sessions within the same subject.

The *ASSR threshold* is defined as the lowest intensity that still produces a ASSR at the corresponding modulation frequency. In the current study this definition is stricter to avoid incorrect threshold estimations. A threshold (in dB SPL) is only accepted if more than half of the intensity levels above this threshold (in steps of 10-dB SPL up to 60-dB SPL) generate a significant response. For example, when stimulus levels at 30- and 40-dB SPL show a response, but those at 50- and 60-dB SPL do not, one does not define a threshold at 30-dB SPL. However, if a response is found at 20-, 30-, and 40-dB SPL, the ASSR threshold is defined at 20-dB SPL. If no threshold can be defined at 60-dB SPL, the ASSR threshold is set to 70-dB SPL.

First, results are shown using SNRs. Next, the justification to convert SNRs to difference scores is presented. The rest of the section presents results using difference scores.

A. Separate channels

For each EEG-channel, Table II displays mean SNRs (and standard deviations) of eight modulation frequencies. Also, root-mean-square (rms) values of the noise are shown for a frequency range between 77 and 115 Hz (modulation frequencies omitted). Intensity of stimulation is 30-dB SPL. Recording length is 32 sweeps after artifact rejection. The table shows means over ten subjects, with test and retest data averaged for each subject (test-retest not significant over all intensities, $p=0.404$, no interactions). For conciseness, values at other intensities (60-, 50-, 40-, 20-, and 10-dB SPL) are not shown.

When comparing 160 difference score values obtained from all eight frequencies and all ten subjects (both test and retest) with 160 corresponding SNRs obtained from all frequencies and all subjects at a specific intensity, the following Spearman correlations r_s are obtained ($p<0.001$): $r_s=-0.110$ (10-dB SPL), $r_s=-0.378$ (20-dB SPL), $r_s=-0.676$ (30-dB SPL), $r_s=-0.707$ (40-dB SPL), $r_s=-0.678$ (50-dB SPL), and $r_s=-0.573$ (60-dB SPL). The strong correlations just above ASSR hearing threshold justify the condensation of six SNR values into a single-valued difference score. This simplifies analyses further on and allows difference scores to be used instead of objectively measurable SNRs. The test-retest statistic for difference scores is not significant ($p=0.439$, no interactions), same for the test-retest statistic of SNRs. As such, difference scores obtained from the same subject can be averaged.

Figure 1 shows mean difference scores (and standard deviations) per EEG-channel for all eight modulated carrier frequencies. Difference scores vary significantly over channels ($p=0.004$). Comparing pairwise (with Bonferroni correction, $p<0.05$), channel 1 has significantly better difference scores than channels 3, 6, 7, and 8; channel 3 has significantly better difference scores than channel 6; channel 4 has significantly better difference scores than channels 7 and 8. There is an interaction between subjects and channels ($p=0.028$). This indicates that a significant difference is present between the best channel of one subject compared to

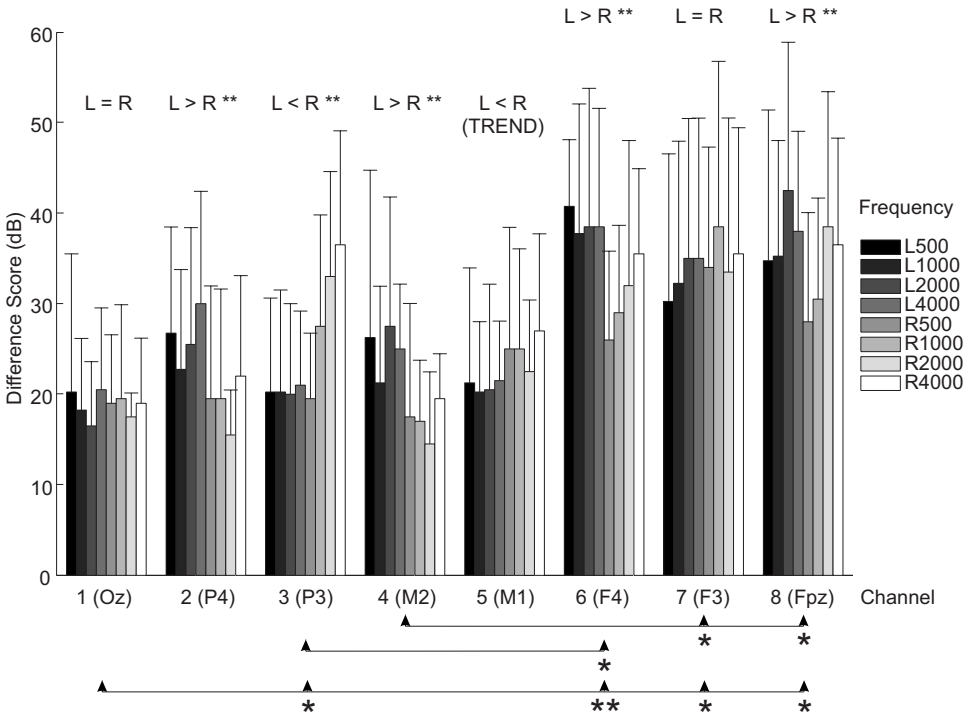


FIG. 1. For each channel from Table I, mean difference scores (and standard deviations) are displayed for all modulated carriers (500, 1000, 2000, and 4000 Hz, left and right). Above each cluster of bars, the relation between carriers applied to the left ear (L) and the right ear (R) is shown. Under each cluster of bars, a comparison between channels is displayed. If a statistical difference is present, this is indicated with * ($0.05 > p \geq 0.01$) and ** ($0.01 > p \geq 0.001$). A trend is considered present if $0.1 > p \geq 0.05$.

the best channel of another subject. Using one particular predefined EEG-channel to optimize recording results cannot be generalized across subjects.

There is no significant difference ($p \geq 0.05$) between frequencies and left-right presentation over all channels. However, there is an interaction effect between channels and left-right application ($p = 0.006$). Figure 1 shows which channels present a significant difference between application to the left ear and application to the right ear. Electrodes placed on the right hemisphere will produce significantly smaller difference scores for carrier frequencies that are applied to the right ear. A similar but somewhat smaller effect can be observed for the left hemisphere. These effects are significantly present on channels 2–4 and 6 and are confirmed on all these channels with six out of ten subjects. Nine out of ten subjects show these effects in at least three out of four significant channels.

If only three out of ten electrodes are available for placement, the best position for the active and reference electrode would be vertex (Cz) and occiput (Oz), respectively, which corresponds to channel 1. This channel returns significantly smaller difference scores than four other channels, including all channels with electrodes on the front side of the head. The side of stimulation is not of significant importance for this channel. This conclusion can also be derived from Table II, where in general higher SNRs are recorded using channel 1.

B. Combination of channels

Section IV A presents data of all individual channels in Table I. This results in a proposal for a channel that records the smallest difference scores. This section discusses the optimal combination of these channels for maximum detection performance (in terms of smallest difference scores), valid for as many subjects as possible and using a minimum number of electrodes. Channels are combined using the detection theory based multi-channel processing technique described in Sec. II. Basically this technique is weighting each channel optimally such that the combined result has the theoretically largest SNR for the ASSR one is looking for (Van Dun *et al.*, 2007b, 2009).

All 255 ($2^8 - 1$) combinations of all eight EEG-channels in Table I are subject to analysis. Channels are combined using Eq. (20). Adding extra channels increases the number of detections. The number of extra channels that can be added is limited however as the number of both true and false detections increases. To keep under control the number of false detections, i.e., detections originating from noise only (which is kept at 5% in this study), detection decision thresholds need to be tightened. In theory, a Bonferroni correction should be applied. In practice, however, this correction proofs too strict. A detection threshold η is calculated using "noise" frequencies with no response present. These noise frequencies are selected close to the modulation frequencies that could contain a response (for example, 1 Hz smaller). To calculate the noise estimate, frequency bins with a response are removed. By selecting the 95 percentile of this distribution of $\Upsilon_A(z)$ values that are calculated on noise frequencies, the practical detection threshold η is found. This is done for all 255 combinations.

For all subjects (both test and retest), difference scores of eight modulated carrier frequencies are calculated for all 255 combinations. No significant difference between test and retest is found ($p = 0.754$). Therefore, for each subject a difference score average is available per frequency and per combination ($10 \times 255 \times 8$ difference scores in total).

Difference scores of most combinations are not normally distributed across subjects. Multivariate analysis requires data with a normal distribution. We follow the nonparametric analysis described in van der Reijden *et al.* (2005), in which

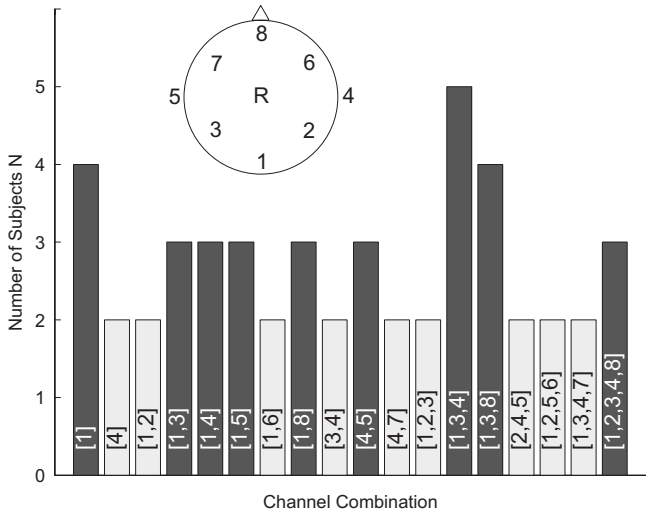


FIG. 2. In Sec. IV B 1, 255 channel combinations per subject are ranked based on each combination's difference score (lowest is best). Difference scores are determined using recorded brainstem responses evoked by left and right stimulus presentations (cf. fourth column of Table III). The top-ten of each list is of interest here. Dark bars represent channel combinations that appear in more than two top-ten lists. Channel combinations appearing only twice in these lists are displayed using light bars. 56 combinations appear only once and are not shown here. Channels are combined using Eq. (20). Only channel combinations represented by dark bars are withheld. These exceed the upper threshold $U=2$, determined using Monte Carlo simulations. The inset represents a scalp viewed from above showing electrode positions from Table I.

outliers are not an issue and equal weights are given to the combinations from each subject regardless of his/her average difference scores.

1. Construction of a top-ten list of combinations

For each subject, a top-ten list is made of combinations with the smallest frequency-averaged difference scores. Five ties are included, limited to the same number of combined channels. For example, when channel combination [1,4,8] is ranked 10th, channel combination [3,6,7] with the same difference score is still included, while channel combination [2,3,4,5] (also with the same difference score) is not, as this combination requires one extra electrode which would be less practical. In this particular case, the top-ten list thus contains 105 combinations. The number of times a particular combination appears in the lists is summed over subjects. This is summarized in Fig. 2. The histogram is subject to further analysis identifying any high ranking combinations that are dominant in all subjects and that will therefore suffice to record the ASSR efficiently.

The average chance level $\bar{d}$ for a specific combination to appear in a subject's top-ten list is $\bar{d}=105/255=0.412$. Monte Carlo simulations are used to find the upper limit U of the 95% confidence interval of the 95 percentile of this distribution d (Press *et al.*, 1992). If this value U can be found, a specific combination only appears more than U times in the top-ten list by chance in less than 5% of the cases. Moreover, this statement has a reliability of 95%. To practically calculate upper limit U, 1000 distributions d_i are constructed. From each distribution d_i, the 95 percentile P_i^{95} is determined. This returns 1000 values P_i^{95}. A 95% confidence interval (and its upper limit U) can be calculated of its mean value $\bar{P}^{95}$.

Each of 1000 distributions d_i, containing (an arbitrarily chosen number of) 5000 instances N_j, is constructed as follows. Out of 255 possible combinations (represented by values between 1 and 255, each corresponding to a particular combination), a random selection S_j of 105 combinations is made. An arbitrary combination c_j is chosen, and the number of appearances N_j of this combination c_j among selection S_j is counted. Instance N_j is one of 5000 instances that distribution d_i consists of. As a validation for this approach, it is confirmed that mean values $\bar{d}_i$ are indeed all close to 105/255. This results in an upper limit U equal to 2. All values above $U=2$ in the histogram of Fig. 2 (depicted by the dark bars) are particular combinations not appearing by chance ($p=0.05$). This is a statement made with a confidence of 95%.

The channel combinations in Fig. 2 that appear more than $U=2$ times in the top-ten list with the smallest difference scores over all subjects are [1] [1,3] [1,4] [1,5] [1,8] [4,5] [1,3,4] [1,3,8] [1,2,3,4,8]. This series is also displayed in the fourth column of Table III. This result seems promising as these combinations generally appear to contain channels with the smallest difference scores (Fig. 1). However, a comparison of test and retest data shows that test-retest reproducibility of combinations in the top-ten list is low. For test data the withheld combinations are [2] [1,2] [1,3] [1,5] [1,6] [1,8] [4,7] [1,2,4] [1,3,7] [1,2,3,4]. For retest data these are [1] [1,3] [1,4] [4,5] [1,3,4]. This non-reproducibility effect is mainly caused by the fact that a large number (i.e., 255) of combinations are candidates for the top-ten list. As a result, even a "promising" combination (one that has a small difference score) might not end up in the top-ten list of both test and retest results due to variations in experiment conditions. By focusing on individual channels appearing in the combinations, this test-retest difference may be reduced, as now only eight channels need to be ranked.

2. Relative contribution of each channel to a top-ten list

The relative contribution of each individual channel to the top-ten lists described in Sec. IV B 1 is an indicator of the importance of each individual channel. For each subject, the number of appearances of a particular channel in the subject's top-ten list is counted and divided by the number of channels in the top-ten list. Test and retest are not significantly different ($p=0.509$, no interactions). Test-retest combined data are displayed per subject in Fig. 3, together with the total relative contribution per channel over all subjects. Relative contribution figures can also be found in the fourth column of Table III. An interesting example shows that "unusable" channels are discarded immediately. During recording of data in the first (test) session, channel 4 from both subjects 2 and 4 suffered severely from muscle artifacts at the right mastoid. No contribution is allowed for channel 4 in these subjects.

Based on the total relative contribution over all subjects,

TABLE III. Step-by-step derivation of most optimal electrode combination for responses originating mainly from the brainstem (Sec. IV B) and mainly from the auditory cortex (Sec. V B). The second row shows all combinations appearing more than $U=2$ times in the top-ten lists for a specific type of stimulation (cf. Fig. 2). The third row depicts the relative contribution and ranking of individual channels to these top-ten lists (cf. Fig. 3). The fourth row indicates the minimum channel set $\mathcal{M}$ needed to cover a certain number of subjects. By adding more channels to a minimal set, more subjects are covered. Here, the minimum channel set $\mathcal{M}_{80}$ covering at least 80% of all subjects (8 out of 10) is depicted in bold and shown separately in the fifth row. This channel set is recommended for practical use.

	Brainstem (80–110 Hz)			
	Left	Right	Combined	Cortex(10 Hz)
Selected combinations ($U>2$)	**[1][1,3]**[1,4] [1,5][1,8][4,5] [1,3,4][1,3,8]	**[1][2][4]** **[1,2][2,4]**[3,4] [4,7]**[1,2,4]**	**[1][1,3][1,4]**[1,5] [1,8][4,5]**[1,3,4]** [1,3,8][1,2,3,4,8]	**[5]**[1,5][4,6]**[5,7]** [2,5,7][4,5,7]**[5,6,7]** **[5,7,8]**[2,5,7,8]**[5,6,7,8]** [4,5,6,7,8][2,4,6,7,8]
Relative contribution (%)	22 11 17 16 13 6 7 8	19 16 12 18 9 11 7 8	23 13 15 16 10 9 6 9	6 10 6 12 25 12 18 11
Channel ranking	1 3 4 5 2 8 7 6	1 4 2 3 6 5 8 7	1 4 3 2 5 6 8 7	5 7 6 4 8 2 3 1
Minimum sets $\mathcal{M}$	{1}–5 **{1,3}–9** {1,3,8}–10	{1}–3 {1,4}–7 **{1,4,2}–8** {1,4,2,3}–9 {1,4,2,3,6}–10	{1}–4 {1,4}–7 **{1,4,3}–10**	{5}–5 {5,7}–6 {5,7,6}–7 **{5,7,6,8}–9** {5,7,6,8,2}–10
Recommended electrodes based on this dataset	{1,3}	{1,4,2}	{1,4,3}	{5,7,6,8}

a ranking can be produced for all eight channels. For the current analysis the channel ranking is 1 4 3 2 5 6 8 7 (cf. Table III). Guided by this ranking, the minimum number of channels can be determined that covers as many top-ten lists as possible. The step-by-step construction of this minimum channel set $\mathcal{M}$ is displayed in Table III. The minimum channel set $\mathcal{M}_{80}$ covering at least 80% of all subjects is depicted in bold. In the fourth column of Table III, at least one of seven combinations that can be made from the set $\mathcal{M}_{80}=\{1,4,3\}$ will appear in ten out of ten (i.e., all) top-ten lists.

When minimum channel set $\mathcal{M}_{80}=\{1,4,3\}$ is determined, the list of selected combinations (with an appearance $U>2$) from the fourth column of Table III can be reduced. Channel combinations from this list that can be formed by $\mathcal{M}_{80}$ are [1] [1,3] [1,4] [1,3,4]. Mean difference scores from these channel combinations range between 18.5 and 19.1 dB ($\pm 1.2-1.5$ dB). Difference scores of all these combinations are not significantly different and are significantly ($p<0.05$) pairwise correlated. As a result, any channel selection out of [1] [1,3] [1,4] or [1,3,4] will result statistically in a minimum mean difference score. To be able to select a channel combination that guarantees a difference score that is always in the top-ten of each subject, three active electrodes should be placed at position 1 (Oz), position 3 (P3), and position 4 (right mastoid), a selection corresponding to minimum set $\mathcal{M}_{80}$. Table IV illustrates this by showing difference scores of each of these four combinations for each subject, together with their ranking compared with all other combinations within that subject.

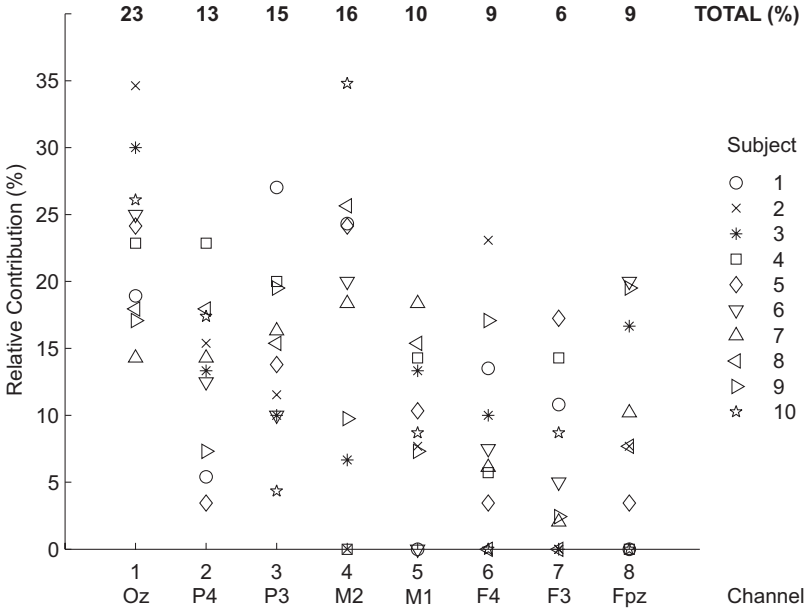


FIG. 3. In Sec. IV B 1, 255 channel combinations per subject are ranked based on each combination's difference score (lowest is best). Difference scores are determined using recorded brainstem responses evoked by left and right stimulus presentations (cf. fourth column of Table III). The top-ten of each list is of interest here. The relative contribution of each of eight channels to each top-ten list per subject is displayed. Additionally, the relative contribution per channel over all subjects is shown.

TABLE IV. Difference scores (dB) are averaged over all eight frequencies for six relevant channel combinations. The rank of each channel combination, relative to all other combinations within the same subject, is given between parentheses. The six channel combinations displayed here are the best combination with the smallest difference score, the worst combination with the largest difference score, and the four combinations selected in Sec. IV B 2. Channel combinations that are present in a subjects's top-ten are highlighted in bold.

Subject	1	2	3	4	5	6	7	8	9	10
Best	14.4 (1)	20.9 (1)	18.1 (1)	13.1 (1)	13.1 (1)	12.5 (1)	16.9 (1)	20.3 (1)	18.4 (1)	10.0 (1)
[1]	21.9 (154)	**22.8 (9)**	**18.1 (1)**	17.5 (58)	14.4 (11)	17.5 (44)	19.3 (83)	25.3 (194)	**20.9 (10)**	**10.0 (1)**
[1,3]	**14.4 (1)**	23.4 (15)	**19.4 (3)**	**13.8 (3)**	15.6 (52)	19.4 (114)	20.0 (134)	23.4 (91)	22.2 (35)	13.8 (23)
[1,4]	20.0 (83)	22.8 (12)	20.6 (13)	20.0 (145)	14.4 (12)	**15.0 (6)**	**18.1 (9)**	22.2 (27)	24.1 (108)	**11.3 (4)**
[1,3,4]	**16.3 (6)**	25.9 (90)	**20.0 (6)**	18.8 (103)	**13.8 (6)**	17.5 (47)	18.1 (15)	**20.9 (3)**	27.2 (188)	**12.5 (10)**
Worst	41.3 (255)	37.2 (255)	53.8 (255)	30.0 (255)	29.4 (255)	33.8 (255)	41.9 (255)	45.9 (255)	52.2 (255)	42.5 (255)

3. Splitting data in left and right stimulus application

To check whether there is a specific reason for the asymmetry in the previous setup, the available data are split according to the two sides of stimulation (left or right). This way, the possible importance of side of stimulation for electrode placement is investigated.

Responses originating from stimuli applied to the left ear are considered separately from those resulting from stimuli applied to the right ear. The procedures from Secs. IV B 1 and IV B 2 are repeated identically.

As shown in the second column of Table III, the minimum set $\mathcal{M}_{80}^{L}$ for stimuli applied to the left ear is $\mathcal{M}_{80}^{L}=\{1,3\}$. This corresponds to active electrodes placed at positions Oz and P3. $\mathcal{M}_{80}^{R}=\{1,4,2\}$ is taken as a minimum set $\mathcal{M}_{80}^{R}$ for stimuli applied to the right ear. Active electrodes should be placed at positions Oz, P4, and the right mastoid. In seven of ten subjects, electrodes on the side of stimulation contribute relatively more to the top-ten lists than the contralateral electrodes. In only one subject, this effect is inverted.

The resulting minimum set $\mathcal{M}_{80}=\{1,4,3\}$ of simultaneous stimuli left and right is a combination of minimum sets $\mathcal{M}_{80}^{L}$ and $\mathcal{M}_{80}^{R}$ of stimuli applied to left and right ears separately. No apparent reason for the asymmetry in $\mathcal{M}_{80}$ can be found however. The asymmetry can be mainly addressed to variability of data across different experiments. When compared with symmetric sets {1,2,3} and {1,4,5}, the sum of relative contributions of single channels from asymmetric set {1,4,3} to top-ten lists is largest in five of ten subjects. Only in one subject, this sum is the smallest. In individual subjects, this asymmetry is thus also present.

C. Artifact robustness

Four different processing methods are considered, two single-channels and two multi-channels. Channel 1 is taken from Table I as the reference channel for single-channel brainstem ASSR measurements with adults (Luts and Wouters, 2005; van der Reijden *et al.*, 2001). Channels 1, 3, and 4 are presented as the minimum set in Sec. IV B 2 and are combined using the multi-channel processing scheme from Sec. II.

The processing schemes are applied on two multi-channel EEG datasets obtained at an intensity of 30-dB SPL. First, they are administered on an EEG dataset with few artifacts ("clean EEG") that is identical to the EEG in Sec. IV A. Second, they are applied on an EEG dataset with a considerable number of artifacts ("dirty EEG"), generated as described in Sec. III A. To calculate a detection threshold η, each of four processing methods below is applied on frequencies without a response (for example, 1 Hz below the modulation frequencies that could contain a response) of artifact-free multi-channel EEG data from Sec. IV A on all intensities. Then, the 95 percentile of this noise distribution is defined as the detection threshold. This way, four different detection thresholds are obtained for each processing method.

1. *Channel 1, normal averaging*. Channel 1 is divided into 32 sweeps (data blocks of 16.384 s) and averaged. Detection is managed using the method described in Sec. II D.
2. *Channel 1, noise-weighted averaging*. Each unfiltered epoch (data blocks of 1.024 seconds) is transformed to the frequency domain using a FFT. Average power P_i between 77 and 115 Hz is computed after removing the power at eight frequencies where responses occur. The time domain epoch is weighted with the average power P_i and concatenated with preceding epochs to form sweeps. Each epoch of the final summed sweep is divided by the sum of the weights $P=\Sigma P_i^{-1}$ of the epochs that have been combined to form that particular epoch [adapted from John *et al.* (2001a)]. Detection is managed using the method described in Sec. II D.
3. Channels 1, 3, and 4 are combined using Eq. (20) with $\boldsymbol{K}_{\text{spat}}$ fixed and $\boldsymbol{K}_{\text{temp}}=\sigma\boldsymbol{I}$ fixed. Mean noise power σ^2 is calculated using Eq. (23) on combined channels 1, 3, and 4.
4. Channels 1, 3, and 4 are combined using Eq. (22) with $\boldsymbol{K}_{\text{spat}}$ fixed. $\boldsymbol{K}_{\text{temp},i}=P_iP\sigma_n\boldsymbol{I}$ is variable and is recalculated for each block i of 8.192 s (this block size returns best results). $\boldsymbol{K}_{\text{temp},i}$ is calculated based on the rationale of noise-weighted averaging. P_i is the average power between 77 and 115 Hz of data block i. P is the sum of the reciprocals of P_i, i.e., $P=\Sigma P_i^{-1}$. Mean noise power σ_n^2 is calculated using Eq. (23) on a noise-weighted average of combined channels 1, 3, and 4.

It is assumed that all responses to the applied stimuli are present in the EEG as the stimulus intensity is 30-dB SPL and hence above the subject's hearing thresholds. This assumption does not guarantee the presence of ASSRs in the EEG however. Adult ASSR thresholds are assumed to lie at

TABLE V. The number of detections (with an assumed maximum of 160) is shown for each processing method described in Sec. IV C. Each processing method is applied to EEG data with few artifacts ("clean EEG") and EEG data with a significant number of artifacts ("dirty EEG"). For methods 1–4, comparisons have been conducted pairwise with Bonferroni correction. Methods 3′, 3″, 4′, and 4″ process two symmetric channel sets but are not used for pairwise comparisons. They are only placed in this table for illustrative purposes.

Method	Description	Clean EEG	Dirty EEG
1	Normal averaging channel 1	117	17
2	Weighted averaging channel 1	122	35
3	$\boldsymbol{K}_{\text{temp}}=\sigma\boldsymbol{I}$ fixed; [1,3,4]	117	57[a]
4	$\boldsymbol{K}_{\text{temp},i}=\boldsymbol{P}_i\boldsymbol{P}\sigma_n\boldsymbol{I}$ var; [1,3,4]	**122**	**72**[b]
3′	$\boldsymbol{K}_{\text{temp}}=\sigma\boldsymbol{I}$ fixed; [1,2,3]	113	31
4′	$\boldsymbol{K}_{\text{temp},i}=\boldsymbol{P}_i\boldsymbol{P}\sigma_n\boldsymbol{I}$ var; [1,2,3]	122	50
3″	$\boldsymbol{K}_{\text{temp}}=\sigma\boldsymbol{I}$ fixed; [1,4,5]	108	44
4″	$\boldsymbol{K}_{\text{temp},i}=\boldsymbol{P}_i\boldsymbol{P}\sigma_n\boldsymbol{I}$ var; [1,4,5]	112	66

[a]Significantly better than approach 1 ($p<0.01$).
[b]Significantly better than approach 1 ($p<0.001$), approach 2 ($p<0.01$), and approach 3 ($p<0.05$).

12 ± 9 dB above hearing threshold for 10-min measurements (Luts and Wouters, 2004). As a result, even for acoustic stimuli that are, for example, 20 dB, above hearing threshold, ASSR presence cannot be guaranteed. However, the different processing schemes are evaluated using identical data sets, eventually eliminating this problem of uncertainty. Hence it is assumed that there are 16 responses available for detection for each subject (test and retest). The maximum number of detections is assumed to be 160. Table V shows the number of detections for each approach: EEG data with few artifacts (clean EEG) and EEG data with a significant number of artifacts (dirty EEG). Test and retest data are not significantly different for both datasets ($p\geq0.67$).

For EEG data with few artifacts, best results are obtained when a noise-weighted averaging approach is used. The improvement relative to normal averaging is not significant however. It does not make a difference if multiple channels are used for processing or just one (reference) channel.

Response detection in EEG data with numerous artifacts is improved significantly when using more than one channel for processing. This improvement can increase significantly again when using a noise-weighted averaging based approach.

In Sec. VI, it is discussed whether a symmetric minimum set would give a more logical electrode placement compared with an asymmetric minimum set. Therefore, for illustrative purposes, Table V adds four extra lines showing the multi-channel processing results of symmetric minimum sets {1,2,3} and {1,4,5}.

V. RESULTS FOR AUDITORY CORTEX ASSRs

This section addresses the following questions:

- What is the most appropriate single EEG-channel to record auditory cortex ASSRs?
- What is the most appropriate combination of multiple EEG-channels to record auditory cortex ASSRs?
- Are above conclusions influenced by the side of stimulation (left or right)?

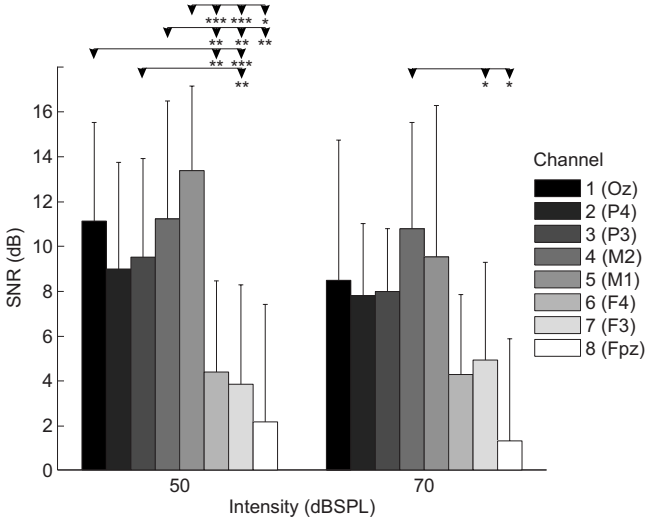


FIG. 4. The mean SNR (and standard deviation) of the 10-Hz response is displayed per channel from Table I. The stimulus is applied to the right ear (next to channel 4) at intensities of 50- and 70-dB SPL. Above each intensity, a comparison between channels is made. If a statistical difference is present, this is indicated with * ($0.05>p\geq0.001$), ** ($0.01>p\geq0.001$), and *** ($0.001>p$).

This section presents results from stimulation at only one ear. Six out of ten subjects are stimulated at the right ear. To preserve symmetry, all electrode positions of the other four subjects are mirrored as if stimulation occurred at the right ear. This swapping operation is allowed as no significant difference ($p=0.904$) in SNR between groups with left ear stimulation and right ear stimulation is found. As a result, Table I refers for this section to the (corrected) side of stimulation as "ipsilateral" and the opposite side as "contralateral."

A. Separate channels

Figure 4 shows mean SNRs (and standard deviations) of the 10-Hz response in all eight channels from Table I for intensities of 50- and 70-dB SPL. Test and retest data are averaged per subject ($p=0.314$, no interactions). There is no significant difference between both intensities ($p=0.113$, no interactions). A main effect between channels is present ($p=0.003$, no interactions). When comparing pairwise (Bonferroni correction) in Fig. 4 at 50-dB SPL, SNRs of channels 4 and 5 are significantly larger than those of channels 6–8. Channel 1 is significantly different from channels 6 and 7. Channel 3 only is significantly different from channel 7. At 70-dB SPL, only SNRs of channel 4 are significantly larger than those of channels 7 and 8. Between subjects an interaction is present with EEG-channels ($p=0.044$). This indicates that the EEG-channel with the largest SNR for one subject is not necessarily the channel with the largest SNR for another subject. The best EEG-channel is subject-dependent.

Due to high variability of SNRs, it is difficult to identify an optimal electrode placement from Table I when only three electrodes are available for placement. From the pairwise comparisons above, channels 4 and 5 (both mastoids) appear to be good choices.

B. Combination of channels

Although no significant difference is present between both intensities in Sec. V A, only the results obtained at 50-dB SPL are focused on. The structure of this section is similar to the structure of Sec. IV. Results at 70-dB SPL are similar and will only be described briefly where different from those at 50-dB SPL.

In Sec. IV, difference scores between ASSR thresholds and behavioral thresholds are used to quantify performance. As no behavioral data are available, only SNRs are used in the analysis, with a minor modification. For example, a response of 12 dB resulting from a five-channel combination is not as convincing as a 12-dB response from a three-channel combination. As a result, the concept of corrected SNR is applicable. The *corrected SNR* is the difference between the SNR of the response and a threshold SNR. The latter increases when more channels are added for combination due to the statistical multiple testing problem. The *threshold SNR* is determined as the SNR that allows 5% false detections when observing a frequency bin without any response present (for example, 1 Hz below the stimulus frequency of 10 Hz). To calculate the noise estimate, frequency bins with a response are removed.

Again, all 255 combinations of all eight EEG-channels in Table I are subject to analysis. Channels are combined using Eq. (20) from Sec. II. No significant difference between corrected SNRs of test and retest data is found ($p=0.805$). Therefore, for each subject an average corrected SNR is available for the 10-Hz response and per combination (10×255 corrected SNRs in total). Corrected SNRs of most combinations do not have a normal distribution across subjects. Therefore, again a top-ten list is made for all subjects. Zero ties are included. The top-ten list thus contains 100 combinations. The number of times a combination appears in this top-ten list is counted (with a mean chance level of $\bar{d}=100/255=0.392$). All combinations appearing more than $U=2$ times in the top-ten list (U as a result of Monte Carlo simulations) are considered not appearing by chance ($p=0.05$), with a confidence of 95%. The withheld combinations for the 10-Hz ASSR are [5] [1,5] [4,6] [5,7] [2,5,7] [4,5,7] [5,6,7] [5,7,8] [2,5,7,8] [5,6,7,8] [4,5,6,7,8] [2,4,5,6,7,8]. They are also displayed in the fifth column of Table III. Only combinations [5] [5,7] [2,5,7] [5,7,8] can also be found in both test and retest results. This nonreproducibility effect is mainly caused by the fact that a large number (i.e., 255) combinations are candidates for the top-ten list. To guarantee test-retest reproducibility, the focus is on the individual channels appearing in these combinations instead. The test-retest difference may be reduced, as now only eight channels need to be ranked.

According to the fifth column of Table III, channels 5 and 7 are by far the channels with highest occurrence in the subjects's top-ten lists. By adding channels 6 and 8, 90% of all subjects are covered. The minimum channel set is thus $\mathcal{M}_{80}=\{5,7,6,8\}$. However, when following the channel ranking of Table III exactly, the minimum set {5,7,6,4} should be the first choice. This minimum set offers the same amount of coverage as {5,7,6,8}, but combination [5,7,6,4] does not appear in the list of withheld combinations however, so channel 8 is chosen instead, and consequently for minimum set {5,7,6,8}.

Based on the minimum channel set $\mathcal{M}_{80}$, only channel combinations [5] [5,7] [5,6,7] [5,7,8] [5,6,7,8] are considered from the list with withheld combinations. Their mean corrected SNRs are between 8.2 and 9.0 dB (±1.1 and 1.2 dB) and not significantly different. They are all significantly pairwise correlated ($p<0.05$). As a result, any channel selection out of these five combinations will result statistically in a maximum mean corrected SNR. To be able to select a channel combination that guarantees a corrected SNR that is always in the top-ten of each subject, however, four active electrodes should be placed at position 5 (contralateral mastoid), position 6 (F4), position 7 (F3), and position 8 (forehead). When data obtained at 70-dB SPL are analyzed, a coverage of 80% is possible with $\mathcal{M}_{80}=\{5,7,6,4\}$, which is similar to the results at 50-dB SPL.

VI. DISCUSSION

All combinations of EEG-channels in this paper are processed using a sufficient statistic that theoretically captures best the amount of useful ASSR target signal present in these EEG-channels. This sufficient statistic originates from the realm of detection theory (Green and Swets, 1966). It can be linked with the multi-channel Wiener filter, an optimal filtering technique which computes an optimal (minimum mean square error) estimate of a reference signal (Scharf, 1991). In the case of ASSR detection, this comes down to a maximization of the SNR of combined channels (Simmer *et al.*, 2001; Van Dun *et al.*, 2007b). This point of view makes it easier to get an idea of what happens when combining EEG data using Eq. (20).

Adding extra data-channels will increase the amount of information that is gathered in the same time period. However, to combine these channels, the use of more advanced signal processing is necessary to truly achieve a performance improvement. If multi-channel data are combined using, for example, simple time domain averaging over channels, the statistical multiple testing penalty will increase the number of false detections proportionally to the number of extra correct detections. By intelligently combining these channels, this multiple testing problem can partly be avoided.

This section discusses results from Sec. V where mainly the brainstem (modulation frequencies between 80 and 110 Hz) and mainly the auditory cortex (10 Hz) are stimulated.

A. Brainstem stimulation

The transition from SNR to difference scores is allowed due to high correlations between both measures. It is assumed that results for one measure can be used for the interpretation of the results of the other measure.

When observing difference scores of reference channel 1 (Cz-Oz), two observations can be made. First, difference scores are slightly elevated compared to other studies. Standard deviations are comparable however (Dimitrijevic *et al.*, 2002; Herdman and Stapells, 2001; Luts and Wouters, 2005;

Picton *et al.*, 2003). The relatively low-noise levels [compared to other studies, like Dimitrijevic *et al.* (2002)] depicted in the rightmost column of Table II are no guarantee for small difference scores. Low-noise levels do not necessarily result in good response detection. Some subjects have very low-noise levels when they sleep, as well as reduced response amplitudes. In these subjects response detection may be easier when they are awake and noise levels are higher (Luts *et al.*, 2008). Therefore, the difference score gap may be caused by the determination method of ASSR hearing thresholds. The determination method in this study appears to be rather strict. However, it is kept identical for the whole study, and final conclusions should not be influenced. Second, although not significantly different, carrier frequencies of 500 and 4000 Hz show a trend of having larger difference scores than 1 and 2 kHz at these intensities, which is also observed in other studies (Dimitrijevic *et al.*, 2002; Herdman and Stapells, 2001; Luts and Wouters, 2004; Picton *et al.*, 1998). Both observations suggest that the data in this study are representative for general brainstem ASSR measurements.

As already indicated in Sec. III, several studies focus on sources of the ASSR with frequencies between 80 and 110 Hz, the frequency region of interest for hearing threshold determination. They concluded that for modulation frequencies above 75 Hz, most of the ASSR is generated in the brainstem. Above 95 Hz, the source lies entirely in the brainstem. These assumptions seem to support the observations made in this paper. When sources are mainly located in the brainstem, smallest difference scores (and largest SNRs consequently) are recorded in electrodes close to the brainstem, on the back of the head and the mastoids. The ipsilateral effect of larger SNRs and smaller difference scores (and thus the optimal combination of electrodes) at the side of stimulus application is partly confirmed by Small and Stapells (2008). They indicated that ASSR amplitudes are significantly smaller at the contralateral side. Difference scores with adults do not differ significantly however. For infants, this ipsilateral effect is reported to be strongly present, both for ASSR amplitudes as ASSR thresholds. This asymmetric effect is also confirmed by van der Reijden *et al.* (2005). This could signify that the orientation of the ASSR sources is stimulus side dependent for adults and especially stimulus dependent for infants. However, the asymmetrical electrode positioning for binaural stimulation cannot be confirmed in literature. The authors assume that results in this paper are due to the used dataset and that a symmetrical electrode placement could be preferred. According to Table V, a recommended symmetric minimum set could be {1,4,5}, only slightly reducing the number of detections for clean EEG as well as dirty EEG. To conclude, van der Reijden *et al.* (2004) reported that a small set of three derivations (Cz-Oz combined with the right mastoid-Cz and the left mastoid-Cz, which corresponds to the minimum set {1,4,5}) yields the best SNR in a larger number of adults than would be expected if all derivations were equally efficient. This result is very similar to the one obtained in this study.

Multi-channel processing does not significantly improve detection performance when it is applied to clean EEG. This shows that most single-channel studies using a Cz-Oz or Cz-neck electrode configuration get close to the best obtainable result [for an extensive overview, we refer to Picton *et al.* (2003)]. The EEG data in these studies are mostly obtained from relaxed adults and sedated children. However, studies that specifically incorporate EEG data with numerous artifacts are rare. Unfortunately, these situations reflect most of the conditions usually observed in a clinical environment. The proposed technique definitely contributes to the ASSR field as it is significantly more robust against artifacts and may improve measurements in these difficult conditions. This improvement can be attributed to the use of specific multi-channel signal processing on multi-channel EEG data. The use of multi-channel EEG measurements is not new (van der Reijden *et al.*, 2004, 2005). However, the application of the multi-channel signal processing strategy described in Sec. II to multi-channel EEG data is a novel approach.

B. Auditory cortex stimulation

As already indicated in Sec. III, when lowering the modulation frequency of the stimulus, the main source of the ASSR shifts more to the auditory cortex, while there is still a source present in the brainstem. This may explain the SNRs being largest on electrodes close to the brainstem (back of the head) and the auditory cortices (both mastoids).

Although no significant differences in SNR are found in Fig. 4 between single electrodes at the ipsilateral and the contralateral mastoid [also reported by Herdman *et al.* (2002)], the dominant channel (contralateral mastoid, channel 5) of the minimum set {5,7,6,8} clearly is located at the opposite side of stimulation. This could be explained by the crossing of the auditory paths beyond the brainstem (Hall, 2007). Extra channels 6–8 of the minimum set {5,7,6,8} lie at the front of the head, contrary to channels with largest SNRs lying at the back of the head, as shown in Fig. 4. This can be explained by the underlying mechanism of the multi-channel processing technique from Sec. II. The combination of weighted channels theoretically has the largest possible SNR (Van Dun *et al.*, 2007b, 2009). For responses originating mainly from the auditory cortex, this result is likely obtained by taking the channel with the largest response (channel 5) and by adding channels that have a small response (channels 6–8) and that have a high-noise correlation with the noise from the channel with the largest response. This observation is in contrast with conclusions in Sec. VI A, which locate the minimum set {1,4,2} in the back of the head for responses originating mainly from the brainstem. The dominant channel for this minimum set is the occiput (channel 1). Any additional channels with small responses (channels 6–8 in front of the head according to Fig. 1) appear to be too remote as noise correlation with these remote channels is presumably too low in the frequency region of interest (80–110 Hz).

VII. CONCLUSION

In this paper, practical performance of a multi-channel EEG processing strategy for ASSR detection based on a detection theory approach is evaluated. Eight-channel measure-

ments of ten normal-hearing adults have been used. First, ASSRs with modulation frequencies between 80 and 110 Hz and mainly originating from the brainstem are considered. It is shown that electrodes should be placed at the back of the head and at mastoids to obtain largest mean SNRs and smallest mean difference scores for individual electrodes. When applying the multi-channel processing strategy, smallest difference scores are found with all subjects when electrodes are placed at five positions: Oz, P3, and right mastoid with Cz as a reference electrode and a ground electrode at, for example, the right clavicle. This combination is significantly more robust against artifacts when compared to a single-channel, three electrode, setup. The number of ASSR detections more than doubles when EEG data with artifacts are considered. Second, ASSRs with a modulation frequency of 10 Hz and mainly originating from the auditory cortex are studied. Again, largest mean SNRs are obtained at single electrodes located at the back of the head and at both mastoids. When applying multi-channel processing, largest mean SNRs for minimum 80% of subjects are obtained when placing electrodes at the contralateral mastoid, F4, F3, and the forehead with Cz as a reference electrode and a ground electrode at, for example, the right clavicle.

ACKNOWLEDGMENTS

This work was supported in part by the Institute for the Promotion of Innovation through Science and Technology in Flanders (IWT-Vlaanderen), in part by FWO Project No. G.0504.04 ("Design and analysis of signal processing procedures for objective audiometry in newborns"), and in part by the Concerted Research Action GOA-AMBioRICS.

Aiken, S. J., and Picton, T. W. (**2008**). "Human cortical responses to the speech envelope," Ear Hear. **29**, 139–157.

Alaerts, J., Luts, H., Hofmann, M., and Wouters, J. (**2009**). "Cortical auditory steady-state responses to low modulation rates," Int. J. Audiol. **48**, 1–12.

Armstrong, M., and Stapells, D. R. (**2007**). "Multiple-stimulus interactions in the brainstem (80 Hz) and cortical (14 & 40 Hz) auditory steady-state responses," in Proceedings of the 20th International Evoked Response Audiometry Study Group (IERASG), Bled, Slovenia, p. 148.

Cebulla, M., Stürzebecher, E., and Elbering, E. (**2006**). "Objective detection of auditory steady-state responses: Comparison of one-sample and q-sample tests," J. Am. Acad. Audiol **17**, 93–103.

Cebulla, M., Stürzebecher, E., and Wernecke, K. D. (**2001**). "Objective detection of the amplitude modulation following response (AMFR)," Audiology **40**, 245–252.

Cohen, L. T., Rickards, F. W., and Clark, G. M. (**1991**). "A comparison of steady state evoked potentials to modulated tones in awake and sleeping humans," J. Acoust. Soc. Am. **90**, 2467–2479.

Dimitrijevic, A., John, M. S., Van Roon, P., Purcell, D. W., Adamonis, J., Ostroff, J., Nedzelski, J. M., and Picton, T. W. (**2002**). "Estimating the audiogram using auditory steady-state responses," J. Am. Acad. Audiol **13**, 205–224.

Dobie, R. A., and Wilson, M. J. (**1996**). "A comparison of t test, f test, and coherence methods of detecting steady-state auditory-evoked potentials, distortion-product otoacoustic emissions, or other sinusoids," J. Acoust. Soc. Am. **100**, 2236–2246.

Drullman, R., Festen, J. M., and Plomp, R. (**1994a**). "Effect of reducing slow temporal modulations on speech reception," J. Acoust. Soc. Am. **95**, 2670–2680.

Drullman, R., Festen, J. M., and Plomp, R. (**1994b**). "Effect of temporal envelope smearing on speech reception," J. Acoust. Soc. Am. **95**, 1053–1064.

Galambos, R., Makeig, S., and Talmachoff, P. J. (**1981**). "A 40-Hz auditory potential recorded from the human scalp," Proc. Natl. Acad. Sci. U.S.A. **78**, 2643–2647.

Green, D., and Swets, J. A. (**1966**). *Signal Detection Theory and Psychophysics* (Wiley, New York).

Hall, J. W. (**2007**). *New Handbook of Auditory Evoked Responses* (Pearson, Boston).

Herdman, A. T., Lins, O., Van Roon, P., Stapells, D. R., Scherg, M., and Picton, T. W. (**2002**). "Intracerebral sources of human auditory steady-state responses," Brain Topogr **15**, 69–86.

Herdman, A. T., and Stapells, D. R. (**2001**). "Thresholds determined using the monotic and dichotic multiple auditory steady-state response technique in normal-hearing subjects," Scand. Audiol. **30**, 41–49.

John, M. S., Dimitrijevic, A., and Picton, T. W. (**2001a**). "Weighted averaging of steady state responses," Clin. Neurophysiol. **122**, 555–562.

John, M. S., Dimitrijevic, A., and Picton, T. W. (**2002**). "Auditory steady-state responses to exponential modulation envelopes," Ear Hear. **23**, 106–117.

John, M. S., Dimitrijevic, A., and Picton, T. W. (**2003**). "Efficient stimuli for evoking auditory steady-state responses," Ear Hear. **24**, 406–423.

John, M. S., Dimitrijevic, A., Van Roon, P., and Picton, T. W. (**2001b**). "Multiple auditory steady-state responses to AM and FM stimuli," Audiol. Neuro-Otol. **6**, 12–27.

John, M. S., and Picton, T. W. (**2000**). "MASTER: A Windows program for recording multiple auditory steady-state responses," Comput. Methods Programs Biomed. **61**, 125–150.

Johnson, D. H., and Dudgeon, D. E. (**1993**). *Array Signal Processing: Concepts and Techniques* (Prentice-Hall, London).

Joint Committee on Infant Hearing (**1995**). "Joint committee on infant hearing 1994 position statement. American academy of pediatrics joint committee on infant hearing," Pediatrics **95**, 152–156.

Kuwada, S., Anderson, J. S., Batra, R., Fitzpatrick, D. C., Teissier, N., and D'Angelo, W. R. (**2002**). "Sources of the scalp recorded amplitude-modulation following response," J. Am. Acad. Audiol **13**, 188–204.

Lins, O. G., and Picton, T. W. (**1995**). "Auditory steady-state responses to multiple simultaneous stimuli," Electroencephalogr. Clin. Neurophysiol. **96**, 420–432.

Luts, H., Desloovere, C., and Wouters, J. (**2006**). "Clinical application of dichotic multiple-stimulus auditory steady-state responses in high-risk newborns and young children," Audiol. Neuro-Otol. **11**, 24–37.

Luts, H., Van Dun, B., Alaerts, J., and Wouters, J. (**2008**). "The influence of the detection paradigm in recording auditory steady-state responses," Ear Hear. **29**, 638–650.

Luts, H., and Wouters, J. (**2004**). "Hearing assessment by recording multiple auditory steady-state responses: The influence of test duration," Int. J. Audiol. **43**, 471–478.

Luts, H., and Wouters, J. (**2005**). "Comparison of MASTER and AUDERA for measurement of auditory steady-state responses," Int. J. Audiol. **44**, 244–253.

Malmivuo, J., and Plonsey, R. (**1995**). *Bioelectromagnetism: Principles and Applications of Bioelectric and Biomagnetic Fields* (Oxford University Press, New York).

Picton, T. W., Durieux-Smith, A., Champagne, S. C., Whittingham, J., Moran, L. M., Giguere, C., and Beauregard, Y. (**1998**). "Objective evaluation of aided thresholds using auditory steady-state responses," J. Am. Acad. Audiol **9**, 315–331.

Picton, T. W., John, M. S., Dimitrijevic, A., and Purcell, D. (**2003**). "Human auditory steady-state responses," Int. J. Audiol. **42**, 177–219.

Picton, T. W., Skinner, C. R., Champagne, S. C., Kellett, A. J., and Maiste, A. C. (**1987**). "Potentials evoked by the sinusoidal modulation of the amplitude or frequency of a tone," J. Acoust. Soc. Am. **82**, 165–178.

Press, W. H., Flannery, B. P., Teukolsky, S. A., and Vetterling, W. T. (**1992**). *Confidence Limits on Estimated Model Parameters in Numerical Recipes in C* (Cambridge University Press, Cambridge), Chap. 15.6, pp. 689–698.

Purcell, D. W., John, M. S., Schneider, B. A., and Picton, T. W. (**2004**). "Human temporal auditory acuity as assessed by envelope following responses," J. Acoust. Soc. Am. **116**, 3581–3593.

Riquelme, R., Kuwada, S., Filipovic, B., Hartung, K., and Leonard, G. (**2006**). "Optimizing the stimuli to evoke the amplitude modulation following response (AMFR) in neonates," Ear Hear. **27**, 104–119.

Saberi, K., and Perrott, D. R. (**1999**). "Cognitive restoration of reversed speech," Nature (London) **398**, 760.

Scharf, L. L. (**1991**). *Statistical Signal Processing: Detection, Estimation and Time Series Analysis*, 1st ed. (Addison-Wesley, New York).

Shannon, R. V., Zeng, F. G., Kamath, V., Wygonski, J., and Ekelid, M.

(**1995**). "Speech recognition with primarily temporal cues," Science **270**, 303–304.
Simmer, K. U., Bitzer, J., and Marro, C. (**2001**). *Post-Filtering Techniques in Microphone Arrays: Signal Processing Techniques and Applications*, edited by M. Brandstein and D. Ward (Springer-Verlag, Berlin), Chap. 3, pp. 39–60.
Small, S. A., and Stapells, D. R. (**2008**). "Normal ipsilateral/contralateral asymmetries in infant multiple auditory steady-state responses to air- and bone-conduction stimuli," Ear Hear. **29**, 185–198.
Stürzebecher, E., Cebulla, M., Elberling, C., and Berger, T. (**2006**). "New efficient stimuli for evoking frequency-specific auditory steady-state responses," J. Am. Acad. Audiol **17**, 448–461.
Stürzebecher, E., Cebulla, M., and Pschirrer, U. (**2001**). "Efficient stimuli for recording of the amplitude modulation following response," Audiology **40**, 63–68.
Valdes, J. L., Perez-Abalo, M. C., Martin, V., Savio, G., Sierra, C., Rodriguez, E., and Lins, O. (**1997**). "Comparison of statistical indicators for the automatic detection of 80 Hz auditory steady state responses," Ear Hear. **18**, 420–429.
van der Reijden, C. S., Mens, L. H. M., and Snik, A. F. M. (**2001**). "Comparing signal-to-noise ratios of amplitude modulation following responses from four EEG derivations in awake normally hearing adults," Audiology **40**, 202–207.
van der Reijden, C. S., Mens, L. H. M., and Snik, A. F. M. (**2004**). "Signal-to-noise ratios of the auditory steady-state response from fifty-five EEG derivations in adults," J. Am. Acad. Audiol **15**, 692–701.
van der Reijden, C. S., Mens, L. H. M., and Snik, A. F. M. (**2005**). "EEG derivations providing auditory steady-state responses with high signal-to-noise ratios in infants," Ear Hear. **26**, 299–309.
Van Dun, B., Rombouts, G., Wouters, J., and Moonen, M. (**2009**). "A procedural framework for auditory steady-state response detection," IEEE Trans. Biomed. Eng. **56**, 1098–1107.
Van Dun, B., Verstraeten, S., Alaerts, J., Luts, H., Moonen, M., and Wouters, J. (**2008**). "A flexible research platform for multi-channel auditory steady-state response measurements," J. Neurosci. Methods **169**, 239–248.
Van Dun, B., Wouters, J., and Moonen, M. (**2007a**). "Improving auditory steady-state response detection using independent component analysis on multi-channel EEG data," IEEE Trans. Biomed. Eng. **54**, 1220–1230.
Van Dun, B., Wouters, J., and Moonen, M. (**2007b**). "Multi-channel Wiener filtering based auditory steady-state response detection," in Proceedings of the International Conference on Acoustics, Speech and Signal Processing (ICASSP) Honolulu, HI, Vol. **II**, pp. 929–932.
van Wieringen, A., and Wouters, J. (**2008**). "LIST and LINT: Sentences and numbers for quantifying speech understanding in severely impaired listeners for Flanders and the Netherlands," Int. J. Audiol. **47**, 348–355.